

Comments on the effects of solution precursor characteristics and thermal processing conditions on the crystallization behavior of sol-gel derived lead zirconate titanate thin films

R. W. Schwartz, J. A. Voigt, and B. A. Tuttle

Sandia National Laboratories, Materials and Process Sciences Center, Albuquerque, New Mexico 87185

D. A. Payne

Department of Materials Science and Engineering, Seitz Materials Research Laboratory, and Beckman Institute, University of Illinois at Urbana-Champaign, Urbana, Illinois 61801

T. L. Reichert and R. S. DaSalla

Sandia National Laboratories, Materials and Process Sciences Center, Albuquerque, New Mexico 87185

(Received 31 January 1996; accepted 14 August 1996)

Lead zirconate titanate (PZT 40/60) thin films were fabricated on electroded silicon wafers using chemical solution deposition. Two different chelating agents, acetic acid and acetylacetone, were used in the synthesis of the precursor solutions. The microstructure of the acetylacetone-derived film was characterized by nucleation at the platinum electrode and a columnar growth morphology ($\sim 100\text{--}200$ nm lateral grain size). In contrast, the acetic acid-derived film was characterized by both columnar grains nucleated at the electrode, and larger ($\sim 1\ \mu\text{m}$) grains nucleated at the surface of the film. Using Fourier transform infrared (FTIR) diffuse reflectance spectroscopy, we also noted that the pyrolysis behavior of the films was dependent on the chelating agent employed. The acetylacetone-derived films, which displayed only one nucleation event, were also characterized by a higher pyrolysis temperature than the acetic acid-derived films. Previously, microstructural differences of this nature were attributed to variations in "precursor structure." In this paper, we discuss an alternative mechanism for the observed microstructural variations in films prepared from different solution precursors. In the model proposed, we discuss how changes in film pyrolysis temperature result in a change in film crystallization temperature, and hence, a change in the effective driving force for crystallization. We show how the change in crystallization driving force is expected to impact the thin film microstructure due to the accompanying variations that occur in the barrier heights for interface (lower electrode) and surface nucleation. A standard approach to nucleation in glasses is used as the basis of the proposed model. Finally, we also discuss how the model can be used to understand the observed effects of heating rate and thickness on the microstructure of solution-derived thin films.

I. INTRODUCTION

Lead zirconate titanate (PZT) thin films have been widely investigated for use in a number of electronic applications including decoupling capacitors,¹ nonvolatile memories,² and optical storage media.³ In the preparation of these materials, chemical solution deposition (CSD) methodologies have been extensively employed. Two of the most widely used approaches are sol-gel processing, which for PZT film deposition usually involves the solvent, 2-methoxyethanol,^{5,6} and hybrid methods, which utilize chelating agents, typically acetic acid, to reduce the hydrolysis rates of the B-site zirconium and titanium alkoxide starting reagents.^{7,8}

It has frequently been observed that the microstructure and degree of orientation of the sol-gel derived ferroelectric thin films are highly dependent on the

chemical precursors and solution preparation conditions employed.⁹⁻¹⁴ Chen and co-workers⁹ studied the degree of orientation of PbTiO_3 (PT) films derived from 2-methoxyethanol solutions that were deposited onto (100) MgO substrates. Although the films were crystallized under identical heat-treatment conditions, they found that films prepared from solutions with low hydrolysis ratios ($r = 2$; where $r = \text{moles H}_2\text{O}/\text{mole metal alkoxides}$) demonstrated a greater degree of (100) orientation than those prepared from solutions with high hydrolysis ratios ($r = 6$). The higher degree of orientation of the $r = 2$ films was attributed to the more weakly branched nature of the precursor species formed under these conditions, and the fact that species of this type should demonstrate easier rearrangement during crystallization. These results are in agreement with those

of Nashimoto and Nakamura¹⁴ who determined that highly (001) oriented PZT 52/48 thin films could be prepared from nonhydrolyzed precursor solutions on MgO. It is also important to note that Chen *et al.*⁹ also observed an effect of film thickness on orientation; as film thickness increased, the degree of orientation decreased.

In the preparation of sol-gel derived LiNbO₃ powders and thin films, Nashimoto and co-workers¹³ also reported a similar impact of *r*-value on crystallization behavior. While Chen *et al.*⁹ observed a decrease in film orientation with increasing *r*-value, Nashimoto and co-workers¹³ noted that films prepared without prehydrolysis grew with a high degree of preferred orientation on sapphire substrates, while films prepared from prehydrolyzed precursors were polycrystalline in nature. Thus, in both of these cases, the importance of the substrate on film nucleation/crystallization behavior was reduced for solutions prepared with higher hydrolysis ratios. It is also worthwhile to note that the crystallization behavior of LiNbO₃ powders depended on *r*-value; higher *r*-values resulted in powders with lower crystallization temperatures.¹³

Kushida and co-workers¹² also investigated the effects of precursor molecular nature on the orientation of PT films derived from 2-methoxyethanol solutions. In their study, they found that films prepared from aged solutions, which should possess larger, and perhaps more highly condensed species, demonstrated a higher degree of orientation than films prepared from fresh solutions. While this result is in apparent contradiction with those discussed above, again, the microstructure of the films was observed to change without a change in the firing conditions; some variation in precursor characteristics was solely responsible for the change in film orientation.

Finally, in addition to the observed variations in film orientation with hydrolysis ratio discussed above, other changes in microstructure as a function of solution preparation conditions have also been reported. Lakeman and Payne¹⁰ have shown that for PZT films typically comprised of small, ~100 nm perovskite grains, the occurrence of large, ~1 μm rosette grains within the uniform fine grain microstructure could be minimized by carefully controlling the solution preparation conditions. It was hypothesized that the observed microstructural differences were due to changes in the oligomeric structure of the precursors obtained under different preparation conditions.

Summarizing the discussion above, the ability to obtain high degrees of orientation during film fabrication has been attributed to (i) the ease of reorientation of weakly branched precursors during crystallization,⁹ or (ii) the alignment of precursor molecules during spin-casting.¹² Precursor structural effects have also been demonstrated to impact other microstructural aspects of

the films, namely, nucleation behavior. We believe that the observed effects of precursor structure on film orientation and microstructure (i.e., films with only columnar grains versus films with both columnar and surface-nucleated grains) are most likely related to one another. However, to tie these observations together, an explanation which goes beyond that of oligomer reorientation during firing, or alignment during deposition, is required.

In this paper, we provide additional insight into defining the characteristics of solution precursors that are important in control of film crystallization behavior. Based on experimental observations and modeling of nucleation barriers, we suggest an alternative explanation for the observed effects of precursor structure on film crystallization behavior. The explanation that we examine is based on the changes in precursor organic nature that result from variations in hydrolysis conditions or additions of chelating agents. We show that these changes induce a change in film pyrolysis temperature, and thereby, film crystallization onset temperature. The change in film crystallization temperature affects the relative driving force for crystallization, and hence, the importance of different nucleation events which serve to define the thin film microstructure.

The development of this type of model should result in an enhanced ability to control thin film orientation and microstructure, permitting the fabrication of films with microstructures tailored for specific applications. For example, the use of PZT films in optical storage devices requires 90° domain switching, which requires large grain size materials. By preparing precursor solutions that have lower nucleation rates, it should be more straightforward to obtain this type of microstructure.

II. EXPERIMENTAL

A. Lead titanate powder preparation and characterization

Lead titanate gel-derived powders were prepared according to the procedure illustrated in Fig. 1. A method developed by Budd *et al.*⁵ was employed for the preparation of a Pb,Ti-methoxyethoxide precursor solution; all reactions were carried out under inert atmosphere conditions using standard Schlenk line techniques. Lead acetate trihydrate (Aldrich Chemical Company, Inc., Milwaukee, WI) was dissolved in HPLC grade 2-methoxyethanol (Aldrich Chemical Company, Inc., Milwaukee, WI) in a 1:8 molar ratio. An "anhydrous" lead acetate precursor was prepared from this solution by three successive distillations. One mole % excess lead was added to the solution to compensate for lead loss during heat treatment. NMR investigations by Ramamurthi and Payne of the structure of this precursor species indicate that dehydration is

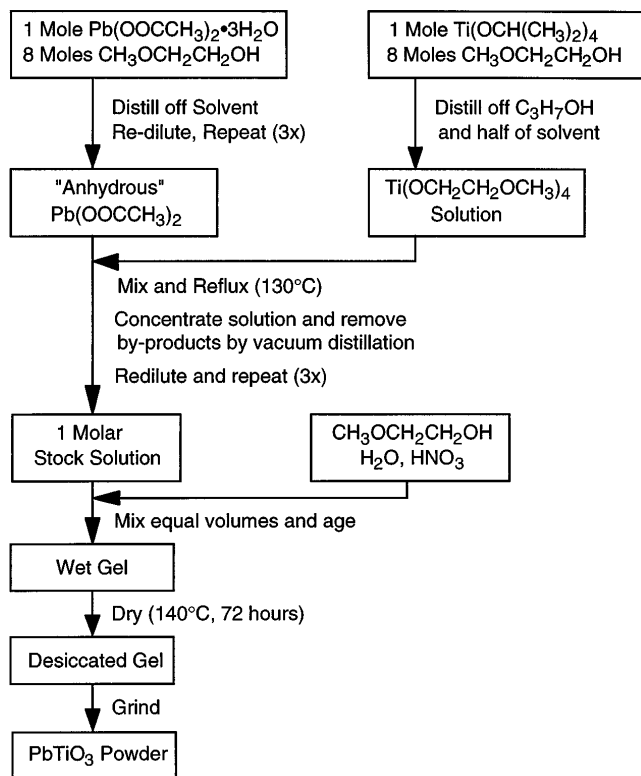


FIG. 1. Flow diagram for the preparation of lead titanate powders by sol-gel processing.¹⁶

not complete and partial exchange of the acetate and 2-methoxyethanol groups occurs, leading to the formation of a $\text{Pb}(\text{OOCCH}_3)(\text{OCH}_2\text{CH}_2\text{OCH}_3) \cdot 0.5\text{H}_2\text{O}$ species.¹⁵

In a separate reaction vessel, a titanium methoxyethoxide precursor was prepared by the reaction of titanium isopropoxide (Aldrich Chemical Company, Inc., Milwaukee, WI) and 2-methoxyethanol (molar ratio 1 : 8) at 125 °C. The by-product of the alcohol exchange reaction was removed by distillation, and the solution concentration was increased to approximately 2.0 M. The Pb and Ti precursor solutions were then combined, refluxed at 130 °C for 60 min, and concentrated by three successive vacuum distillations at ~50 °C to prepare the PbTiO_3 precursor solution. After the final vacuum distillation, the solution was cooled to 25 °C and diluted in a volumetric flask to yield a 1.0 M PT precursor solution. Solution concentration and Pb/Ti ratio (actual ~1.02/1.00) were confirmed by atomic absorption spectroscopy.¹⁶ Studies by Ramamurthi and Payne¹⁵ and Coffman and Dey¹⁷ have indicated that after combination of the lead and titanium solutions, the acetate groups of the lead precursor are almost completely removed, and the solution species is essentially alkoxide in nature.

Bulk lead titanate gels (0.5 M) were formed by combining equal volumes of the 1.0 M stock solution and a 2-methoxyethanol solution containing water and catalyst. Water additions, i.e., r , the molar ratio of water

to complex alkoxide, were varied from 2 to 4. The final concentration of the HNO_3 catalyst (Fisher Scientific, Pittsburgh, PA) was 0.1 M. Gelation times varied from 12 s to 22 h depending on the hydrolysis ratio. After gelation, gels were aged for 30 min at 25 °C, and were then dried at 140 °C for 72 h. The gels were then lightly pulverized using an agate mortar and pestle.

The weight loss and pyrolysis behavior of the gel-derived powders were studied by thermal gravimetric analysis (Du Pont 1090 thermal analyzer with TGA module), and surface areas of the gel-derived powders were measured by nitrogen adsorption experiments (Micromeritics ASAP 2400). All samples were degassed overnight at 125 °C under vacuum prior to surface area measurement.

B. Lead zirconate titanate thin film deposition and characterization

The precursor solutions for PZT thin film fabrication were prepared by an Inverted Mixing Order (IMO) method which has been previously described.^{18–20} The 0.4 M solutions were synthesized by first adding titanium isopropoxide to zirconium *n*-butoxide-butanol (Aldrich Chemical Company, Inc., Milwaukee, WI) while stirring. Purified acetic acid (Fisher Scientific, Pittsburgh, PA), ~4 moles/mole alkoxide, was then added, followed by the addition of methanol (Fisher Scientific, Pittsburgh, PA) and lead (IV) acetate (Aldrich Chemical Company, Inc., Milwaukee, WI). After heating to ~85 °C for dissolution of the lead reagent, solution preparation was completed with further additions of methanol, acetic acid, and water. Generally, 50 ml batches were prepared, and 10 to 15 mole % excess lead reagent was added to compensate for PbO volatility during heat treatment. For selected samples, 3 moles acetylacetone (acac; 2,4-pentanedione) (Fisher Scientific, Pittsburgh, PA) per mole PZT were added to the precursor solution approximately 15 min prior to film fabrication.

The organic content of the precursor species was determined by converting the deposition solutions to powders by vacuum distillation of the solvent and by-products at 25 °C. Carbon and hydrogen levels of the dried powders were then measured with a Perkin-Elmer 2400 Series II CHNS/O Elemental Analyzer. Organic content of the (300 °C) pyrolyzed films was studied by diffuse reflectance FTIR spectroscopy (Nicolet Magna 550 with DRIFTS attachment).

Thin films were deposited by spin-casting onto Pt/Ti/SiO₂/Si substrates (Silicon Quest International, Santa Clara, CA) at 3000 rpm for 30 s. After deposition, the films were heated on a hot plate at 300 °C for 5 min for pyrolysis of organic species. Fired layer thickness was between 900 and 1000 Å per layer, depending

upon acac addition. Thicker films were prepared by a multilayering approach, with a crystallization heat treatment after every fourth layer, unless otherwise specified. Crystallization was achieved by heat treatment at 650 °C for 30 min, using a ramp rate of 20 °C/min. To further investigate transformation behavior, additional samples were prepared at intermediate heat-treatment temperatures (500–600 °C) by heating at 20 °C/min and quenching. X-ray diffraction analysis was accomplished using a Siemens D500 diffractometer (Cu K α); identical instrumental conditions were employed for all samples.

III. RESULTS AND DISCUSSION

A. Precursor rearrangement effects on thin film orientation

Before discussing the results of the present study and why it may be worthwhile to consider alternative explanations for the observed effect of solution precursor variations on film crystallization behavior, it is important to consider the previously postulated explanations for this relationship. Chen *et al.*⁹ proposed that weakly branched precursors were required for the preparation of oriented films, while Kushida and co-workers¹² proposed that chain-like species were required. Both research groups cited changes in “precursor structure” as being responsible for the decrease in film orientation that occurred with water additions⁹ or solution aging.¹²

We feel that there is compelling evidence which suggests that while this effect may play a role, it may not necessarily be the key mechanism that causes the change in the ability to prepare highly oriented films. If the precursor structure truly is critical, we should perhaps expect that it would only be possible to prepare highly oriented films from the one solution preparation route that generates precursors with the required structure. However, this is simply not the case; highly oriented PT and PZT thin films have been prepared using a variety of solution deposition routes. Figure 2 presents the results of Tuttle *et al.*²¹ and Nashimoto and Nakamura¹⁴ which demonstrate that highly oriented films may be prepared using a variety of deposition routes. Tuttle *et al.*²¹ used an acetate route to deposit their thin films, while Nashimoto and Nakamura¹⁴ used the 2-methoxyethanol route. Research that has focused on the structure of the precursor species formed in these different routes suggests that the species are quite different. For example, studies of the precursors formed in the 2-methoxyethanol process indicate a relatively low ratio of acetate to alkoxide species,^{15,17} while studies of the species formed in the acetate method indicate a high ratio of acetate to alkoxide species.¹⁹ Since the species generated in these different processes possess such different structures, yet both may be used to successfully deposit highly oriented

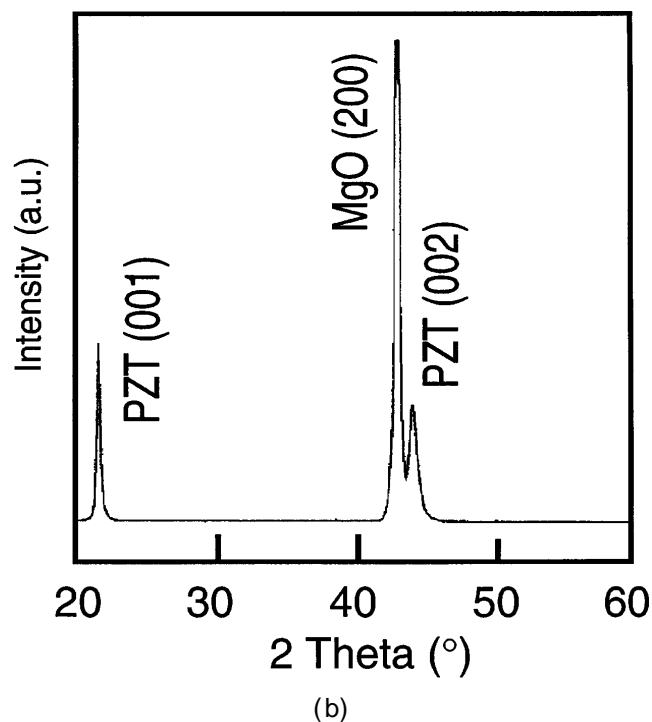
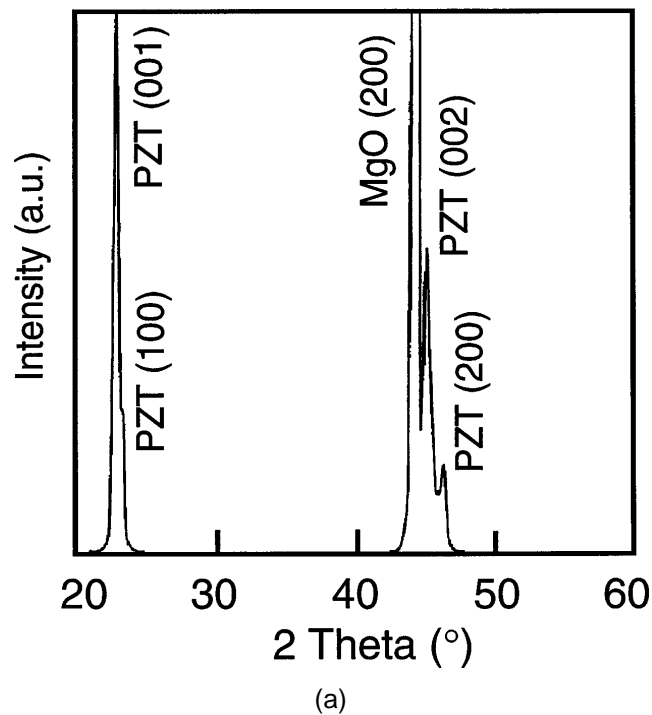


FIG. 2. Comparison of oriented thin films prepared by two chemical solution deposition methods: (a) Tuttle *et al.*²¹ (a hybrid preparation route based on the use of acetic acid), and (b) Nashimoto and Nakamura¹⁴ (a sol-gel process utilizing 2-methoxyethanol).

thin films, we question whether precursor structural differences can be solely responsible for the observed variations in film orientation with water addition or solution aging.

We therefore feel that other, more general characteristics of the precursors may be responsible for the observed variations. We propose that changes in the pyrolysis behavior of the species that accompany changes in solution hydrolysis ratio may be the cause of changes in film orientation, and other observed variations in film crystallization behavior.²⁰ Before considering the change in the pyrolysis behavior of films derived from 2-methoxyethanol solutions prepared with different r -values, and the role pyrolysis behavior may play on the ability to prepare oriented thin films, we discuss the importance of pyrolysis behavior on thin film microstructure for films derived from an acetate-based solution deposition process.

B. Relationship between precursor pyrolysis and thin film nucleation behavior

In addition to the observed orientation differences discussed above, other effects of precursor nature on thin film microstructure have also been noted.^{10,20} A typical example of these effects is shown in Fig. 3, for films prepared from (a) an aged, IMO acetate precursor solution, and (b) an aged, IMO acetate precursor solution that has been modified by the addition of a second, stronger chelating ligand, acetylacetone. While both microstructures are essentially 100% perovskite in nature, as determined by x-ray diffraction, the film prepared from the “standard” acetate route [Fig. 3(a)] displays a microstructure consisting of columnar, ~ 100 – 200 nm perovskite grains nucleated at the lower electrode, and ~ 1 μm semispherical perovskite grains nucleated at the thin film surface. We have also observed that the density of the surface-nucleated grains increases with solution aging; films prepared from fresh solutions display very few surface-nucleated grains, while those prepared from aged solutions display a high density of the larger surface grains.

In contrast to the film prepared from the aged solution, the film prepared from the acetylacetone modified (aged) solution [Fig. 3(b)] displays a microstructure resulting from only nucleation of columnar grains at the lower electrode; the surface nucleation event has been completely eliminated. We have previously demonstrated that this improvement in microstructure results in improved ferroelectric properties, and a dramatic decrease in optical scattering losses.¹¹

To understand the improvement in thin film microstructure obtained through the addition of acetylacetone, we have studied the organic content and pyrolysis behavior of the two thin film precursors, and have coupled

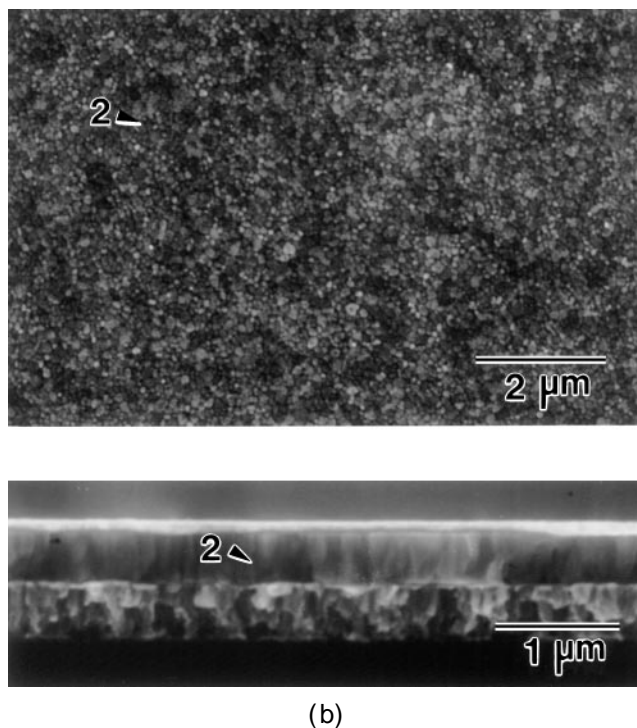
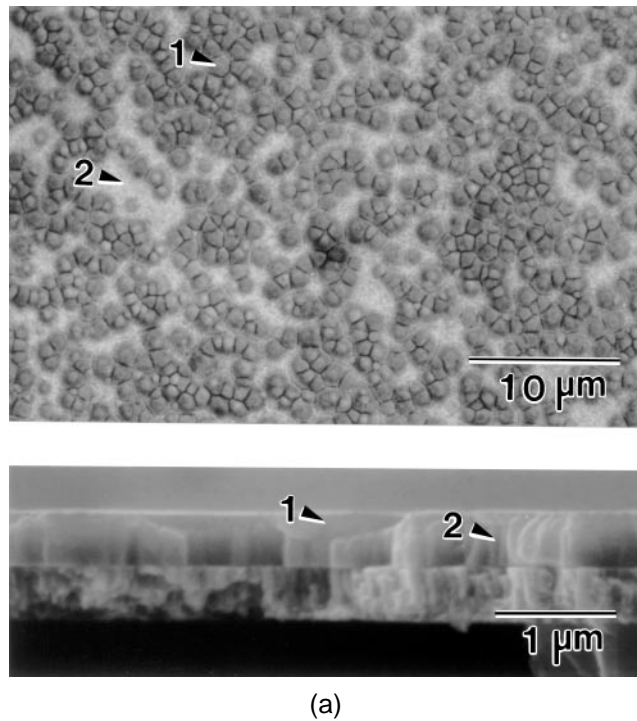


FIG. 3. (a) Plan-view and cross-sectional SEM photomicrographs of 4-layer PZT 40/60 thin films prepared from (a) an aged IMO solution, and (b) the same aged IMO solution to which acetylacetone (acac; 3 moles/mole PZT) was added immediately prior to film fabrication. For cross-sectional views: lower layer—Pt bottom electrode; second layer—PZT thin film; upper layer—Pt top electrode [(b) only]. (1) Surface-nucleated, larger perovskite grains; (2) Interface-nucleated, smaller columnar perovskite grains.

this analysis with traditional nucleation theory for crystallization from glasses. The organic content of the standard acetate and acetylacetonone modified precursors was studied by elemental analysis, and the pyrolysis behavior of the corresponding films was investigated using diffuse reflectance FTIR spectroscopy. Elemental analysis of the two precursors indicated that addition of acetylacetonone to the solution resulted in precursor species with the expected higher organic contents. The species formed in the standard acetate process had 16.23%C and 2.27%H, while the species formed in the acetylacetonone modified process were characterized by 20.07%C and 2.53%H.

Perhaps of greater importance than the change in organic content, the pyrolysis behavior of the films was also affected by the acetylacetonone addition. Figure 4 shows FTIR spectra of the standard IMO and acac-modified IMO films following pyrolysis (i.e., organic removal by heat treatment in an oxidizing environment) at 300 °C. Three main bands are observable in the spectra as follows: metal-oxygen (M–O) bonding: 400–800 cm^{-1} ; carbon-oxygen (C–O) bonding: 1300–1700 cm^{-1} ; and entrapped CO_2 at $\sim 2370 \text{ cm}^{-1}$.²² The C–O bonding region is indicative of organic content in the films, due either to the presence of residual acetate or acac species. In the standard IMO process [Fig. 4(a)], a heat-treatment temperature of 300 °C is sufficient to remove the bulk of the organic

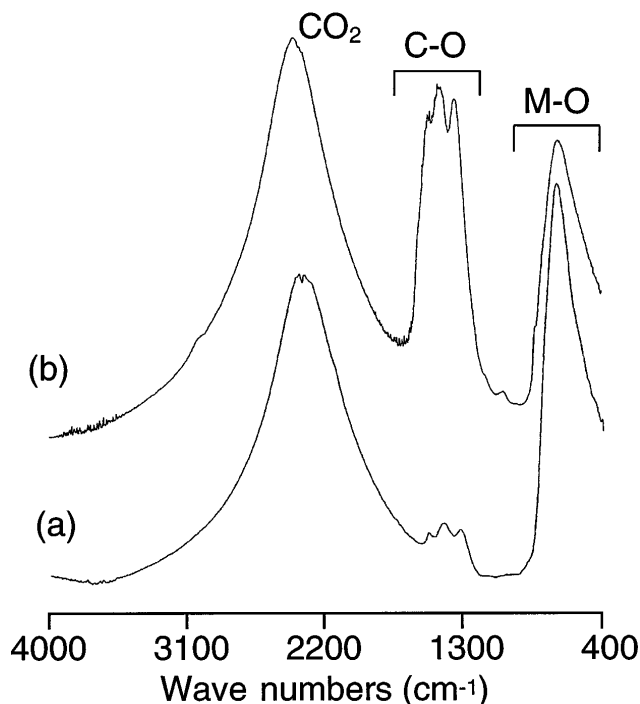


FIG. 4. Diffuse reflectance FTIR spectra of 4-layer PZT 40/60 thin films heat-treated at 300 °C for 5 min on a hot plate: (a) standard IMO and (b) acac-modified IMO.

components of the film prior to the crystallization anneal. However, the modification of the IMO precursor species by acetylacetonone results in incomplete pyrolysis at this temperature, as indicated by the intense C–O stretching bands at $\sim 1400 \text{ cm}^{-1}$ [Fig. 4(b)]. Thus, higher pyrolysis temperatures are required for acetylacetonone-derived films compared to films prepared by the standard acetate process. This result is in agreement with studies of zirconia films prepared from acetate and acetylacetonone-based precursors; films prepared from the acetylacetonone precursor displayed higher pyrolysis temperatures.²³

The importance of this result is that, frequently, in sol-gel derived materials, it has been observed that the onset of crystallization occurs at temperatures slightly greater than the pyrolysis temperature. For example, in sol-gel derived zirconia thin films, it was observed that films that displayed higher pyrolysis temperatures also displayed higher crystallization temperatures.²³ In the lead titanate system, the effects of acetylacetonone additions on crystallization temperatures were studied by Shih and Lu.²⁴ They found that sol-gel derived powders prepared without acetylacetonone crystallized into the perovskite phase at $\sim 455 \text{ °C}$, whereas powders prepared with 2 moles acetylacetonone per mole of PT only crystallized at a temperature of $\sim 475 \text{ °C}$. Based on this result, the observed impact of acetylacetonone additions on the crystallization temperature of our zirconia films,²³ and the change in the pyrolysis behavior of the PZT films of the present study, we would predict that the acetylacetonone-modified IMO films of the present study would undergo crystallization at a higher temperature than the acetate derived (standard IMO) films.

We have investigated this hypothesis by heat-treating films prepared by the two methods to temperatures between 500 and 600 °C and conducting x-ray diffraction analysis. Results are presented in Fig. 5 for films which have been heated to 560 °C at 20 °C/min and quenched by removing from the furnace. Comparing the intensity of the diffraction peaks for these films, it may be seen that crystallization into the perovskite phase is significantly more advanced in the standard IMO film than in the acac-modified IMO film. The (100) and (111) perovskite diffraction peaks of the standard IMO film are approximately three to four times as intense as those of the acac-derived film. Other evidence of the more advanced crystallization of the standard IMO film is also evident in this figure; namely, the higher order diffraction peaks [(200) and (201)] of the standard IMO film are significantly sharper than for the acac-derived film. Thus, as observed for ZrO_2 films and PbTiO_3 powders, in the present study, the addition of acac to the precursor solution delays the film crystallization process to higher temperatures.

By studying the impact that this change in crystallization temperature has on the driving forces that

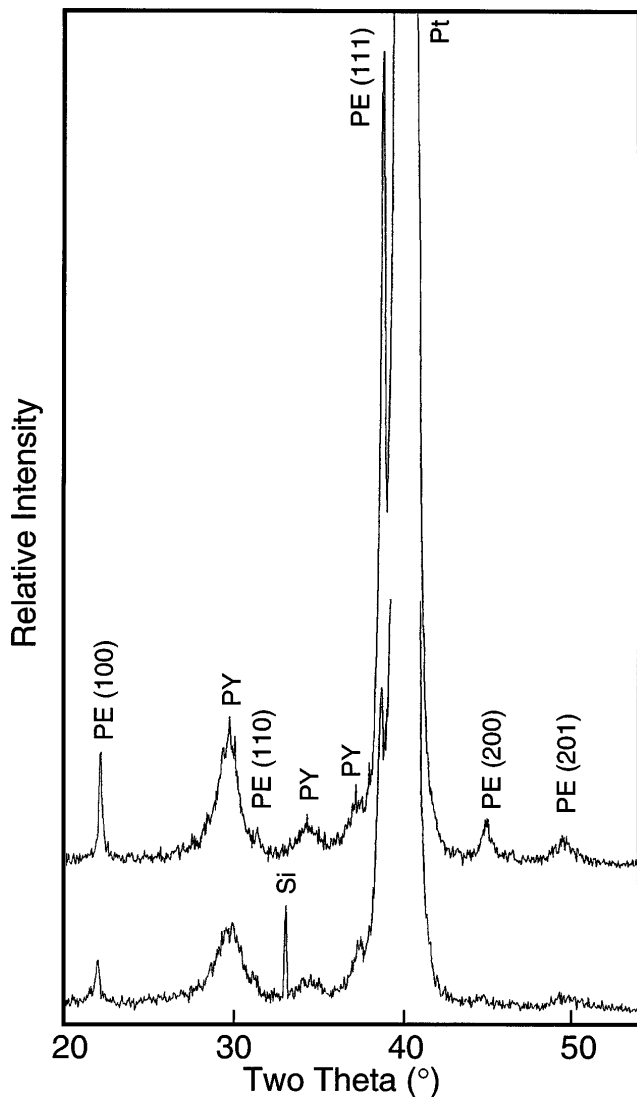


FIG. 5. X-ray diffraction spectra of (a) aged IMO and (b) acac-modified IMO PZT 40/60 thin films heated to 560 °C at 20 °C/min and quenched; PE = perovskite peaks and PY = pyrochlore peaks. Peaks for substrate components are also indicated.

define crystallization, a second explanation may be proposed that accurately describes both the microstructural variations resulting from acac addition, as well as the observed effects of hydrolysis content on film orientation presented previously by Chen and co-workers.⁹ Shown in Fig. 6 is a schematic diagram of the relative free energies of the crystalline perovskite phase, the supercooled liquid, and the amorphous, sol-gel derived thin film.^{25,26} The excess free energy of the amorphous, sol-gel derived film compared to the supercooled liquid is due to the higher surface area, excess structural free volume, and higher hydroxyl content of the film.²⁵

In our transformation model, the line drawn for the crystalline phase is for perovskite, and we treat the amorphous → perovskite transformation as a single step

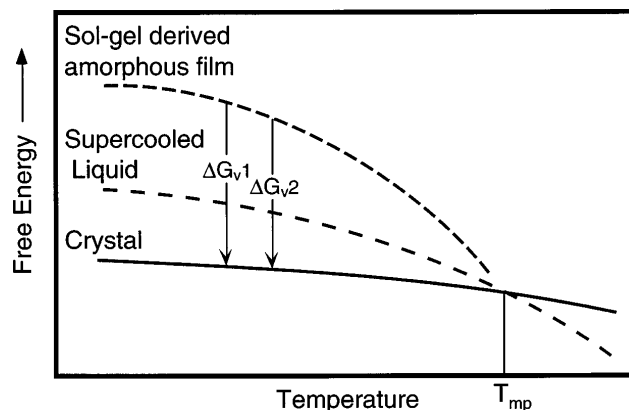


FIG. 6. Schematic diagram of the free energies of a sol-gel derived amorphous film, the ideal supercooled liquid, and the crystalline perovskite phase.^{25,26} $\Delta G_{v,1}$: crystallization driving force for low pyrolysis temperature precursors; $\Delta G_{v,2}$: driving force for high pyrolysis temperature precursors.

process. Intermediate phases, i.e., pyrochlore or fluorite, have been stabilized under certain heat-treatment conditions, and solution-deposited films are typically believed to transform via one of these intermediate phases,^{27,28} as shown in Fig. 5. However, thermal analysis of the transformation of sol-gel derived powders by Differential Scanning Calorimetry (DSC) or Differential Thermal Analysis (DTA) has never displayed separate exothermic events for the amorphous → fluorite and fluorite → perovskite transformations; only a single exothermic event for the amorphous → perovskite conversion has ever been observed.^{16,24} Therefore, although it may not be entirely correct to view this transformation as a single step process, since intermediary fluorite-type phases have been observed, thermal analysis seems to lend some credence to this approach. Treating the transformation in this manner also simplifies the analysis.

Through examination of Fig. 6, it may be seen that the transformation of the amorphous film that crystallizes at a lower temperature is driven by a larger free energy difference between the film and the crystalline phase than the film that transforms at a higher temperature. Since this free energy difference defines the barrier heights for heterogeneous nucleation at the interface and the surface, as well as the barrier height for homogeneous nucleation within the bulk of the film, a change in the driving force for crystallization will impact the relative barrier heights for these different nucleation events.

It is possible to understand how this effect may impact the relative importance of the different nucleation events by using standard nucleation theory. Consider what happens to the energy barriers for homogeneous and heterogeneous nucleation when the driving force for nucleation is changed, as would occur for different transformation temperatures. Equations (1) and (2) describe the free energy barriers for homogeneous (ΔG_{homo}^*) and

heterogeneous ($\Delta G_{\text{hetero}}^*$) nucleation, respectively:

$$\Delta G_{\text{homo}}^* = \frac{16\pi\gamma^3}{3(\Delta G_v)^2}, \quad (1)$$

$$\Delta G_{\text{hetero}}^* = \frac{16\pi\gamma^3}{3(\Delta G_v)^2} \cdot f(\theta), \quad (2)$$

where γ is the interfacial energy, ΔG_v is the driving force for crystallization, i.e., the free energy difference per unit volume for the amorphous film-crystalline film transformation, and $f(\theta)$ is a function related to the contact angle θ according to Eq. (3),

$$f(\theta) = \frac{2 - 3 \cos \theta + \cos^3 \theta}{4}. \quad (3)$$

As the driving force for crystallization ΔG_v decreases, the barriers for both homogeneous and heterogeneous crystallization increase; however, due to the $f(\theta)$ contact angle term, they do not increase by the same amount. TEM studies of the early stages of nucleation in solution-derived PZT 20/80 thin films on MgO substrates by Voigt and co-workers indicated contact angles of $\sim 90^\circ$.²⁹ Due to similar lattice matching between PZT and Pt, our lower electrode material, we also assume a contact angle of 90° . Therefore, $f(\theta) = 0.5$. Making the further assumptions that γ is invariant with precursor chemistry, and the increase in crystallization temperature for the films which display higher temperature pyrolysis results in a 10% decrease in the driving force; then, from Eqs. (1) and (2), we find that the difference in the barrier heights for homogeneous and heterogeneous crystallization, $\Delta(\Delta G_{\text{homo}}^* - \Delta G_{\text{hetero}}^*)$ is increased by

24%. Thus, for precursor systems which display higher pyrolysis and crystallization temperatures, nucleation events other than nucleation at the substrate interface become less attractive during conversion to the crystalline ceramic. (Typically, nucleation at the substrate is the most energetically favorable nucleation event for films deposited on substrates with a reasonable degree of lattice matching.)

The impact of this effect on crystal nucleation behavior is illustrated schematically in Fig. 7, where the barrier heights for heterogeneous and homogeneous crystallization are compared to a hypothetical thermal input used for crystallization. For precursor films that display higher pyrolysis temperatures [Fig. 7(b)], a single heterogeneous nucleation event can dominate the thin film microstructure because other nucleation events are energetically not favorable with the given thermal input. However, for films that display lower pyrolysis temperatures [Fig. 7(a)], the thermal input during heat treatment may be adequate to surmount the energy barriers for both heterogeneous and homogeneous nucleation, leading to a microstructure defined by more than one nucleation event.

While Fig. 7 is perhaps the simplest way to illustrate the considerations that govern the transformation process, it should be noted that this schematic probably depicts an exaggeration of the differences between the actual energy barriers that dictate crystallization behavior. This occurs because in the present case, the final microstructure [Fig. 3(a)] is not defined by heterogeneous and homogeneous nucleation, but is defined by two different heterogeneous nucleation events: nucleation at the electrode and at the film surface. Therefore, the larger,

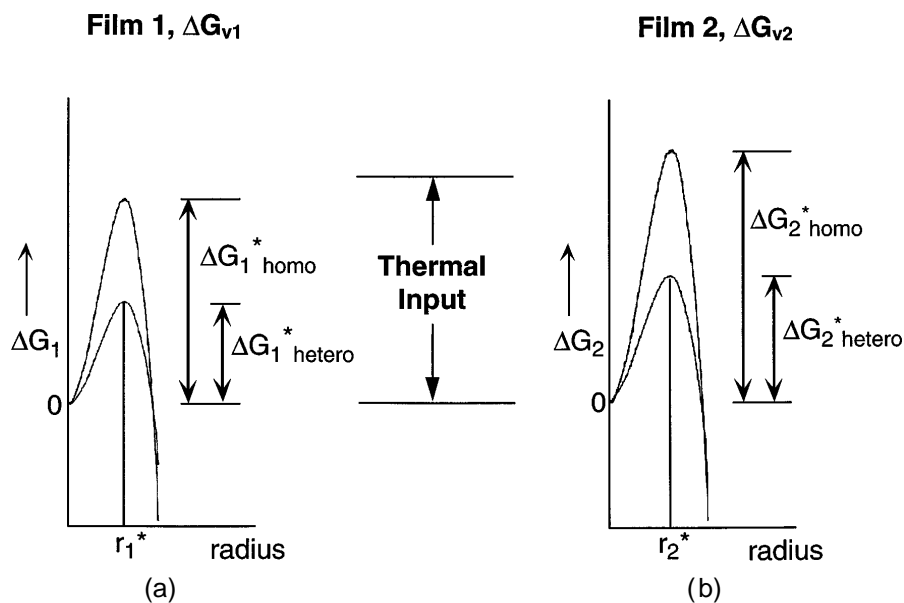


FIG. 7. Hypothetical free energy barriers for homogeneous and heterogeneous nucleation in thin films prepared from (a) low pyrolysis temperature precursors and (b) high pyrolysis temperature precursors. r_1^* and r_2^* represent the critical radii for nuclei growth.

homogeneous nucleation energy barrier illustrated would also be lowered by an $f(\theta)$ term; i.e., a barrier should be shown for a second, energetically less favorable, heterogeneous nucleation event.

In addition to this change, one further modification to this simple model is also required. Because nucleation (and grain growth) in these films commences not during the crystallization hold, but during heating to the anneal temperature, the anneal (or hold) temperature represents a thermal input that is greater than the barrier heights illustrated in either scenario of Fig. 7. Therefore, the microstructures of the films are defined not only by the energy barriers which describe the different nucleation events, but also by the kinetics which govern the grain growth associated with these different nucleation events.

A schematic that illustrates the interrelationships between kinetic effects, i.e., heating rate, and the thermodynamic barriers for crystallization is presented in Fig. 8. Here, the barrier heights are shown for two heterogeneous nucleation events: interface nucleation [$f(\theta) = 0.5$] and surface nucleation [$f(\theta) = 0.75$, assumed]. We assume a larger $f(\theta)$ term for (external) surface nucleation, because nucleation at this surface is somewhat less favorable than nucleation at the "lattice matched" lower electrode, but should be more favorable than true homogeneous nucleation. Again, in deriving this figure, a 10% decrease in driving force was used for the higher crystallization temperature case [Fig. 8(b)].

In Fig. 8, we consider the relationship between heating rate and the energy barriers for nucleation. It

may be seen that for films heated at identical rates, the times (or temperatures) at which the nucleation events take place are defined by the energy barriers governing the different nucleation events; lower energy barrier nucleation events occur at lower temperatures, or at earlier times, during heating. While the heating rate illustrated was chosen arbitrarily, analogous results are obtained for other heating rates. We can also see in this figure that the low energy barrier nucleated grains have an opportunity (a finite time window) for growth prior to subsequent nucleation events which may occur at higher temperatures, when the thermal input is sufficient to surmount the energy barriers for these nucleation events (i.e., heterogeneous nucleation at the surface or homogeneous nucleation within the bulk of the film). However, it is important to note that the time available for growth prior to subsequent nucleation events is dependent on the energy barriers; films crystallizing with higher driving forces have a smaller time for growth prior to the second nucleation event.

We now return our attention to the observed changes in thin film microstructure shown in Fig. 3 caused by the addition of acetylacetone to the solution. Recall that the acac-modified films had higher pyrolysis and crystallization temperatures, as illustrated in Figs. 4 and 5.²⁴ Using the model of Fig. 8 to explain the observed microstructural variations of the present study, the acac-modified film [Fig. 3(b)] may be considered to be represented by the situation illustrated on the right half of Fig. 8, i.e., Film 2. Nucleation occurs at the interface

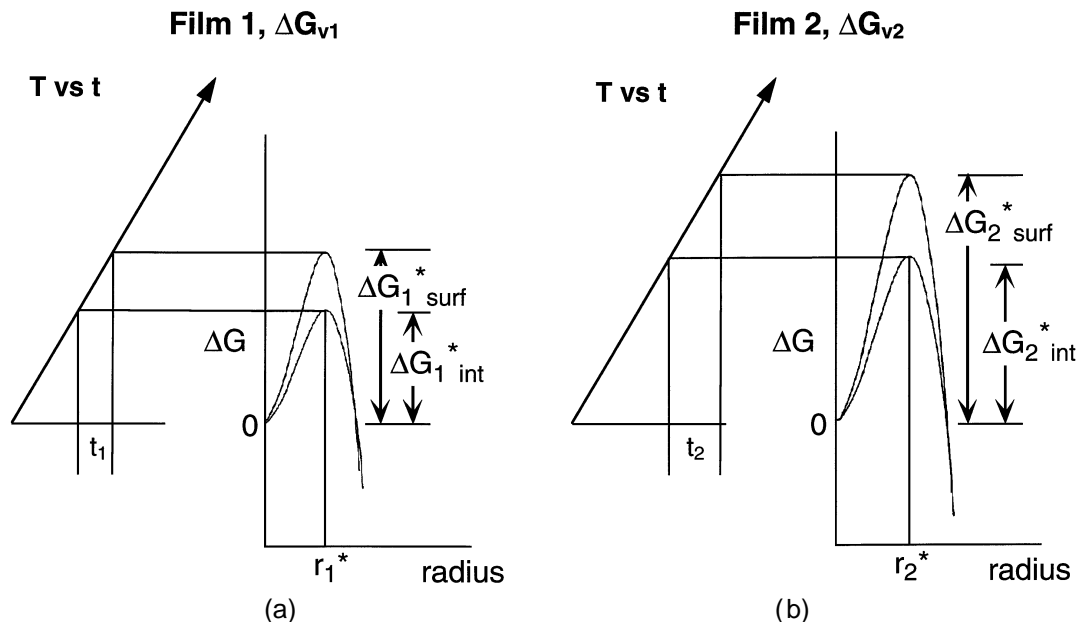


FIG. 8. Relationship between the heating rate used during the crystallization heat treatment and the free energy barriers for nucleation at the electrode interface and the film surface; (a) low pyrolysis temperature and (b) high pyrolysis temperature precursors. Note that the time between the interface and surface nucleation events for the higher pyrolysis temperature scenario (t_2) is greater than for the case of lower temperature pyrolysis (t_1). r_1^* and r_2^* represent the critical radii for nuclei growth.

and columnar grains start to grow toward the external surface of the film. Although the temperature continues to increase toward the point where surface nucleation might occur, the heating and grain growth rates are such that sufficient time is available for the interface-nucleated grains to completely consume the amorphous phase, prior to the onset of surface nucleation. The outcome is a columnar microstructure dictated by a single nucleation event, and is primarily due to the magnitude of the difference in the energy barriers for interface and surface nucleation that are present for higher crystallization onset temperatures.

In contrast, the film prepared from the aged IMO solution [Fig. 3(a)] undergoes pyrolysis and crystallization at lower temperatures. Thus, the amorphous \rightarrow perovskite transformation of this film is governed by thermodynamic barriers for crystallization that are less different in magnitude than for the acac-derived film. Therefore, even though interface nucleation initially occurs in this film, there is less time for the growth of these grains prior to the onset of surface nucleation. This may be seen in Fig. 8 where t_1 is less than t_2 . In the present case, t_1 is apparently insufficient to allow for the grains nucleated at the interface to completely consume the amorphous phase prior to the onset of surface nucleation. The result is a microstructure that displays two nucleation events: columnar perovskite grains nucleated at the lower electrode and larger perovskite grains nucleated at the surface of the film. Thus, even though the same anneal temperature was used for film fabrication, changes in the thermodynamic barriers for nucleation, due to differences in film pyrolysis and crystallization temperatures of the standard and acac-derived films, completely changed the nature of the resulting microstructure by changing the relative importance of the different nucleation events.

Based on the model of Fig. 8, we would predict that film thickness and heating rate would also have significant effects on film microstructure. Changes in heating rate are predicted to affect microstructure because the time between the different nucleation events is changed, as is the time for grain growth following the initial nucleation event. Our preliminary investigations indicate that variations in thin film microstructure caused by changes in heating rate do indeed fit the proposed model of Fig. 8; slower heating rates yielded films with columnar microstructures dictated by a single interface nucleation event, whereas faster heating rates, which allow less time for growth of the initially nucleated grains, display both interface and surface nucleation.³⁰ For the films prepared at the slower rate, sufficient time is apparently allowed for complete transformation of the film (via nucleation at the electrode and growth) prior to the thermal input equaling the energy barrier associated with surface nucleation, and initiating nucleation at this

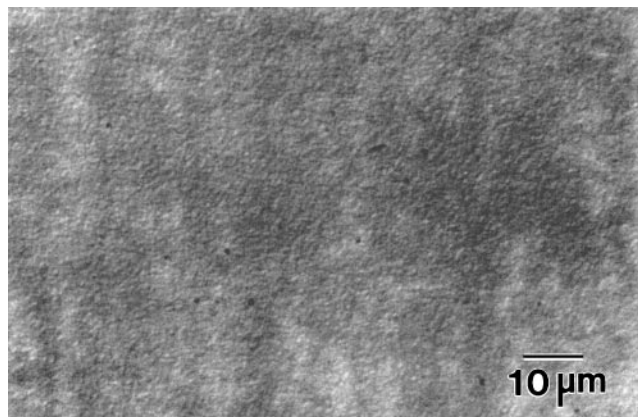
location. The microstructures of these films strongly resembled the one shown in Fig. 3(a).

In contrast, films prepared at the faster heating rate had microstructures displaying both interface and surface nucleation, and the films strongly resembled the film illustrated in Fig. 3(b). For these films, because of the faster heating rate, the energy barrier for surface nucleation is evidently surmounted prior to completion of the transformation via the initial nucleation event, and the resultant microstructure is therefore defined by multiple nucleation events. We are continuing our evaluation of these films because changes in heating rate also cause a change in pyrolysis kinetics, which complicates this analysis somewhat.

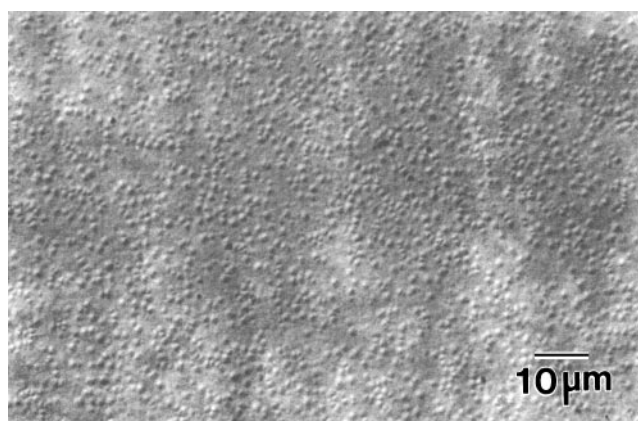
Fortunately, it is more straightforward to evaluate the effect of film thickness on microstructure, and to compare these results with the predictions of Fig. 8. Based on our model, film thickness effects on microstructure are expected due to the change in the time required for the growth of the interface-nucleated grains to consume the amorphous film. The time required for the growth of the interface-nucleated grains to reach the surface is less in thinner films than in thicker films. Because of this effect, surface nucleation of perovskite grains should be less pronounced in thinner films. Figure 9 demonstrates this effect for 2- and 5-layer films prepared by a standard IMO process. The 2-layer film displays essentially no surface-nucleated grains, while the 5-layer film displays a high density of the large surface-nucleated perovskite grains.

C. Relationship between precursor pyrolysis behavior and thin film orientation

We now return our attention to the effects of hydrolysis conditions on the orientation of the 2-methoxyethanol derived PT thin films prepared by Chen *et al.*⁹ In addition to the changes in precursor structure which may occur with changes in hydrolysis conditions, consider what happens to the organic content and the pyrolysis behavior of the precursor species. As the hydrolysis level is increased, precursors with greater extents of condensation, and thereby, lower organic contents are prepared.^{16,31} Figure 10 illustrates this effect for sol-gel derived PT powders prepared by the 2-methoxyethanol process using acidic catalysis conditions. As the hydrolysis ratio is increased from 2.5 to 3.5, the organic content of the powders decreases from $\sim 24\%$ to $\sim 8\%$. In addition, and perhaps more importantly, the pyrolysis temperature of the powders decreases from $\sim 480^\circ\text{C}$ to $\sim 300^\circ\text{C}$. The lower pyrolysis temperatures of the more highly hydrolyzed precursors should allow for crystallization to proceed at lower temperatures than in systems prepared using lower hydrolysis ratios. Thus, in the study of Chen *et al.*,⁹ as demonstrated above,



(a)



(b)

FIG. 9. Optical plan-view photomicrographs of (a) 2-layer and (b) 5-layer PZT 40/60 thin films. Note that the thicker film shows a much higher density of surface-nucleated grains.

a difference in the thermodynamic driving force for crystallization may again be responsible for the observed differences in crystallization behavior, rather than a change in the precursor structure. Using the model proposed in Figs. 7 and 8, the lower degree of orientation of the high r films prepared by Chen and co-workers⁹ may simply be attributable to the fact that, as crystallization temperature is decreased, the relative importance of the nucleation event at the substrate is decreased and other nucleation events become energetically more favorable.

Chen and co-workers⁹ also noted that film orientation decreased with increasing film thickness. Again, it is possible to explain this observation based on the model presented in Fig. 8. In thicker films, a longer time period is required for the growth of the interface-nucleated grains to consume the amorphous matrix during the transformation. Because of this, a higher temperature is reached prior to the completion of the transformation process, which allows for the occurrence of other, more energetically intensive, nucleation events. These other

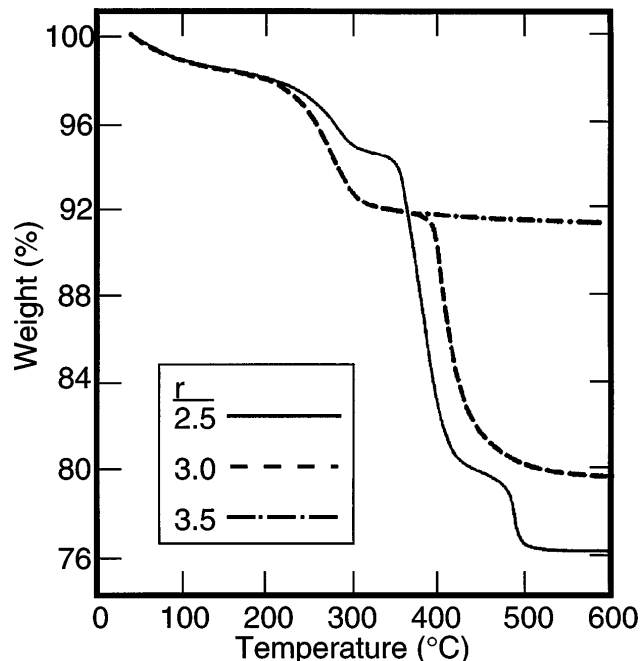


FIG. 10. TGA spectra of 2-methoxyethanol derived PbTiO_3 powders prepared under acidic hydrolysis conditions; r = moles H_2O /mole PbTiO_3 .¹⁶

nucleation events result in grains of other orientations, which reduces the overall degree of (100) orientation of the film.

The model proposed in the present study may also be used to explain the results of Nashimoto and co-workers for sol-gel derived LiNbO_3 thin films.¹³ These investigators noted that films prepared without prehydrolysis grew with preferred orientation on sapphire substrates, while films prepared from prehydrolyzed precursors were polycrystalline in nature. While no substantial changes in crystallization temperature were noted for the films prepared on sapphire substrates, significant changes in the crystallization temperatures for sol-gel derived powders ($\sim 100^\circ\text{C}$), as well as films deposited on Si ($\sim 50^\circ\text{C}$), were observed to result from changes in the level of prehydrolysis.¹³ As expected, as the prehydrolysis level was increased, the crystallization temperatures of these samples were observed to decrease. Thus, since a 50°C crystallization temperature range ($350\text{--}400^\circ\text{C}$) is quoted for the films prepared on sapphire, similar, but smaller, changes in film crystallization temperature versus prehydrolysis level may be responsible for a change in the driving force for crystallization. Because of this change, we would expect the importance of interface nucleation in defining film orientation and microstructure to be reduced, and it would be reasonable for the films to change from highly oriented to polycrystalline in nature as the level of prehydrolysis is increased.

D. Other film physical properties which may impact crystallization

Before concluding, it is worthwhile to note that other changes in the nature of thin films with hydrolysis ratio may also impact their transformation behavior. As an example, we consider the changes in surface area that result from variations in hydrolysis conditions, and how such variations may potentially impact film crystallization behavior. Shown in Fig. 11 are the effects of hydrolysis and catalysis conditions on the surface area of 2-methoxyethanol derived PT powders. It may be seen that as the hydrolysis ratio is increased, the surface area of the powders increases.

Variations in surface area are important because the surface area, free volume, and residual hydroxyl content of a material serve to define the excess free energy (i.e., the position of the free energy curve) of the amorphous film compared to the equilibrium supercooled liquid.²⁵ Materials with higher surface areas are expected to possess higher free energies. In an analogous fashion to changes in crystallization temperature, this variation might thus also affect the driving force for crystallization, and therefore, the relative importance of various nucleation events.

Based on the effects of r value on the surface areas of PT powders shown in Fig. 11, we might predict that the films of Chen *et al.*⁹ prepared with higher r -values would also have higher surface areas. These films would therefore again possess an excess driv-

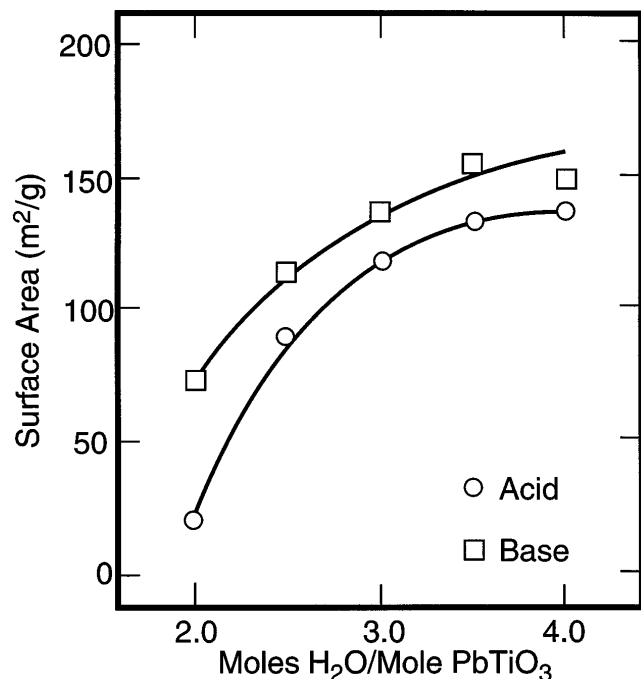


FIG. 11. Surface areas of 2-methoxyethanol derived PbTiO_3 desiccated gels prepared under different hydrolysis and catalysis conditions.¹⁶

ing force for crystallization compared to the lower r -value films, and an energy barrier diagram resembling Fig. 7(a), rather than Fig. 7(b) would result. The expected outcome in this scenario would again be the preparation of films with a lower degree of orientation, due to the probability of multiple nucleation events.

Thus, alternative explanations for the effects of hydrolysis conditions on film crystallization behavior which adequately describe the observed results may also be hypothesized. At this time, however, little direct evidence exists that documents the possible relationship between properties such as film surface area and crystallization behavior. In contrast, considering the results of the present study, as well as those of previous investigators, there appears to be compelling evidence which suggests that a link exists between pyrolysis/crystallization temperature and the crystallization behavior of the films.

Finally, we should also mention that in addition to variations in pyrolysis behavior, other changes in the properties of the films resulting from changes in solution preparation conditions may also contribute to observed differences in thin film microstructure. For example, changes in solution chemistry that induce variations in lead retention, amorphous structure, fluorite ordering, impurity level, defect content, and nucleation site density within the bulk of the film may also play a role in defining thin film microstructure. As with surface area, however, the specific impact of such variations on film microstructure has not been investigated.

IV. CONCLUSIONS

In previous reports on the effects of solution chemistry variations on thin film microstructure and orientation, differences in "precursor structure" were frequently cited as being responsible for the observed variations. In the present paper, we have proposed a model that demonstrates that the observed microstructural and orientational variations may be more closely related to changes in film pyrolysis behavior induced by changes in solution preparation conditions, i.e., hydrolysis ratio or use of chelating agents. The model is based on the fact that changes in film pyrolysis temperature can cause changes in crystallization temperature, which in turn, alter the driving force governing the transformation. Using standard nucleation and growth theory, we have demonstrated how the variation in driving force causes a change in the thermodynamic barriers that define the active nucleation mechanisms, and thereby, the microstructure or degree of orientation of sol-gel derived PZT thin films. By employing this model, it should be possible to determine the solution preparation and thermal processing conditions that are most effective at generating highly oriented thin films with uniform microstructures.

ACKNOWLEDGMENTS

The portion of this work performed at Sandia National Laboratories was supported by the U.S. Department of Energy under Contract No. DE-AC04-94AL85000. The authors would like to thank D. Dimos of Sandia National Laboratories and J.S. Speck of the University of California at Santa Barbara for enlightening discussions. The authors would also like to acknowledge the technical support of R.G. Tissot and G. Zender.

REFERENCES

1. D. Dimos, S.J. Lockwood, R.W. Schwartz, and M.S. Rodgers, IEEE Trans. on Components, Packaging, and Manufacturing Tech. A **18**, 174 (1995).
2. J.F. Scott and C.A. Paz de Araujo, Science **246**, 1400 (1989).
3. C.E. Land, J. Am. Ceram. Soc. **71** (11), 905 (1988).
4. R.W. Vest and J. Xu, Ferroelectrics **93**, 21 (1989).
5. K.D. Budd, S.K. Dey, and D.A. Payne, Brit. Ceram. Soc. Proc. **36**, 107 (1985).
6. C.D.E. Lakeman, J-F. Campion, and D.A. Payne, in *Ferroelectric Films*, edited by A.S. Bhalla and K.M. Nair (Ceramic Trans. **25**, American Ceramic Society, Westerville, OH, 1992), pp. 413–439.
7. G. Yi, Z. Wu, and M. Sayer, J. Appl. Phys. **64** (5), 2717 (1988).
8. R.W. Schwartz, B.C. Bunker, D.B. Dimos, R.A. Assink, B.A. Tuttle, D.R. Tallant, and I.A. Weinstock, Integrated Ferro. **2**, 243 (1992).
9. C. Chen, D.F. Ryder, Jr., and W.A. Spurgeon, J. Am. Ceram. Soc. **72** (8), 1495 (1989).
10. C.D.E. Lakeman and D.A. Payne, J. Am. Ceram. Soc. **75** (11), 3091 (1992).
11. R.W. Schwartz, T.J. Boyle, S.J. Lockwood, M.B. Sinclair, D. Dimos, and C.D. Buchheit, Integrated Ferro. **7**, 259 (1995).
12. K. Kushida, K.R. Udayakumar, S.B. Krupanidhi, and L.E. Cross, J. Am. Ceram. Soc. **76** (5), 1345 (1989).
13. K. Nashimoto, M.J. Cima, P.C. McIntyre, and W.E. Rhine, J. Mater. Res. **10**, 2564 (1995).
14. K. Nashimoto and S. Nakamura, Jpn. J. Appl. Phys. **33**, Pt. 1, No. 9B, 5147 (1994).
15. S. Ramamurthi and D.A. Payne, J. Am. Ceram. Soc. **73** (8), 2547 (1990).
16. R.W. Schwartz, Ph.D. Thesis, University of Illinois (1989).
17. P.R. Coffman and S.K. Dey, J. Sol-Gel Sci. Technol. **1**, 251 (1994).
18. R.W. Schwartz, R.A. Assink, and T.J. Headley, in *Ferroelectric Thin Films II*, edited by A.I. Kingon, E.R. Myers, and B.A. Tuttle (Mater. Res. Soc. Symp. Proc. **243**, Pittsburgh, PA, 1992), pp. 245–254.
19. R.A. Assink and R.W. Schwartz, Chem. Mater. **5** (4), 511 (1993).
20. R.W. Schwartz, R.A. Assink, D. Dimos, M.B. Sinclair, T.J. Boyle, and C.D. Buchheit, in *Ferroelectric Thin Films IV*, edited by S.B. Desu, B.A. Tuttle, R. Ramesh, and T. Shiosaki (Mater. Res. Soc. Symp. Proc. **361**, Pittsburgh, PA, 1995), pp. 377–387.
21. B.A. Tuttle, J.A. Voigt, D.C. Goodnow, D.L. Lamppa, T.J. Headley, M.O. Eatough, G. Zender, R.D. Nasby, and S.M. Rodgers, J. Am. Ceram. Soc. **76** (6), 1537 (1989).
22. D.M. Haaland, Sandia National Laboratories, private communication. In previous studies with sol-gel derived alumina, a broad resonance at $\sim 2300\text{ cm}^{-1}$ was attributed to entrapped CO_2 . The width of the resonance was believed to be due to the distribution of pore sizes within the material.
23. R.W. Schwartz, J.A. Voigt, T.J. Boyle, T.A. Christenson, and C.D. Buchheit, Ceram. Eng. Sci. Proc. **16** (5), 1045 (1995).
24. W-H. Shih and Q. Lu, in *Amorphous Insulating Thin Films*, edited by J. Kanicki, W.L. Warren, R.A.B. Devine, and M. Matsumura (Mater. Res. Soc. Symp. Proc. **284**, Pittsburgh, PA, 1993), pp. 481–486.
25. C.J. Brinker and G.W. Scherer, in *Ultrastructure Processing of Ceramics, Glasses, and Composites*, edited by L.L. Hench and D.R. Ulrich (John Wiley & Sons, Inc., New York, 1984), pp. 43–59.
26. R. Roy, J. Am. Ceram. Soc. **52**, 344 (1969).
27. B.A. Tuttle, T.J. Headley, B.C. Bunker, R.W. Schwartz, T.J. Zender, C.L. Hernandez, D.C. Goodnow, R.J. Tissot, and J. Michael, J. Mater. Res. **7**, 1876 (1992).
28. A.P. Wilkinson, J.S. Speck, A.K. Cheetham, S. Natarajan, and J.M. Thomas, Chem. Mater. **6** (6), 750 (1994).
29. J.A. Voigt, B.A. Tuttle, T.J. Headley, and D.L. Lamppa, in *Ferroelectric Thin Films IV*, edited by S.B. Desu, B.A. Tuttle, R. Ramesh, and T. Shiosaki (Mater. Res. Soc. Symp. Proc. **361**, Pittsburgh, PA, 1995), pp. 395–402.
30. R.W. Schwartz and T.L. Reichert, unpublished results.
31. R.W. Schwartz, D.A. Payne, and A.J. Holland, in *Ceramic Powder Processing Science*, edited by H. Hausner, G.R. Messing, and S. Hirano (Deutsche Keramische Gesellschaft, 1989), pp. 165–172.